GEOLOGY | THE GEOLOGICAL SOCIETY OF AMERICA®

https://doi.org/10.1130/G49344.1

Manuscript received 31 May 2021
Revised manuscript received 18 August 2021
Manuscript accepted 23 August 2021

Published online 2 November 2021

Oceanic strike-slip faults represent active fluid conduits in the abyssal sub-seafloor

Christian Hensen[1], Florian Scholz[1], Volker Liebetrau[1], Norbert Kaul[2], Marianne Nuzzo[3], Mark Schmidt[1], Luis Batista[4], Heinrich Villinger[2] and Pedro Terrinha[4,5]

[1]GEOMAR Helmholtz Centre for Ocean Research Kiel, Wischhofstraße 1-3, 24148 Kiel, Germany
[2]Faculty of Geosciences, Bremen University, Klagenfurter Straße 2-4, 28359 Bremen, Germany
[3]Integrated Geochemical Interpretation Ltd., Hallsannery, Bideford, Devon EX39 5HE, UK
[4]Instituto Portugues do Mar e da Atmosfera (IPMA), Rua C-do Aeroporto, 1749-077 Lisbon, Portugal
[5]Instituto D. Luiz (IDL), Universidade de Lisboa, Campo Grande, 1749-016 Lisbon, Portugal

ABSTRACT

We present pore-fluid geochemistry and heat-flow data along the SWIM1 fault in the Horseshoe Abyssal Plain (northeastern Atlantic Ocean). The SWIM1 fault is part of the transcurrent plate boundary between Africa and Eurasia and cuts through as much as 5-km-thick sediments overlying >140 Ma oceanic lithosphere. In a number of places, restraining segments (as long as 15 km) of the SWIM1 fault generate anticlines (positive flower structures) that protrude as ~100-m-high hills above the abyssal plain. Heat flow and gradients of dissolved constituents in pore water are enhanced at these seafloor highs. Transport-reaction modeling confirms that slow advection of deep-seated fluids, depleted in Mg and enriched in Sr and CH_4, can explain the observations. The geochemical signature is similar to the one observed at deep-sea mud volcanoes located eastward on the SWIM1 fault. The upward-migrating fluids have interacted with carbonate rocks at maximum 5 km depth, which represent the oldest sedimentary unit on top of the basement. We argue that deep-rooted fluids can generally be mobilized and transported upward along flower structures that formed in restraining-bend segments of long strike-slip faults. Such tectonic settings represent largely unrecognized corridors for mass exchange between lithosphere and ocean.

INTRODUCTION AND GEO-TECTONIC CONTEXT

The Horseshoe Abyssal Plain (HAP) and the Gulf of Cadiz (northeastern Atlantic Ocean) host the easternmost segment of the Azores-Gibraltar fracture zone (Fig. 1), which is characterized by prominent strike-slip faults (southwest Iberian margin [SWIM] faults). The SWIM faults constitute a diffuse plate boundary between Africa and Eurasia, which intersects the accretionary wedge west of Gibraltar (Zitellini et al., 2009). The basement in this region consists of exhumed mantle (Martínez-Loriente et al., 2013), normal oceanic crust, and hyperextended continental crust (Ramos et al., 2017). In the Gulf of Cadiz, several mud volcanoes (MVs) are located along these faults, particularly at intersections with thrust faults (Magalhães et al., 2012). MV fluids have been shown to be strongly affected by water-rock interactions. On the accretionary wedge (Fig. 1), the fluids are predominantly derived from clay-mineral dehydration (illitization of smectite), implying that they are freshened with respect to normal seawater and enriched in fluid-mobile elements such as Li and B (Hensen et al., 2007; Scholz et al., 2009; Vanneste et al., 2011). Proximal to the African continental slope, illitization signals are commonly overprinted by the leaching of evaporites (Haffert et al., 2013), while pre-leaching chlorinity levels can be reconstructed using $\delta^{18}O$ values of pore fluids (Hensen et al., 2007). With increasing distance from the coast, the degree of freshening gradually declines, revealing a decreasing importance of illitization (Scholz et al., 2010). This applies particularly to the Porto MV as well as the Abzu–Tiamat–Michael Ivanov (ATI) MVs in Horseshoe Valley west of the deformation front (Fig. 1) and is in accordance with the thinning of Cenozoic terrigenous sedimentary units, which are the predominant source of clay (Scholz et al., 2010). At these MVs, fluids show a strong imprint of non-radiogenic Sr, predominantly derived from Upper Jurassic carbonates, which form the oldest stratigraphic unit on top of the basement. Due to the specific combination of Sr and B enrichments and Sr isotopic signals, admixing of a minor fraction of basement-derived water was deduced (Hensen et al., 2015), a conclusion further corroborated by numerical modeling analyses (Schmidt et al., 2018). The tapping of the old formation water suggests the existence of active, deep-reaching fluid pathways. In fact, fault systems cutting through the Mesozoic rift units have previously been described based on seismic records (Terrinha et al., 2009).

In this study, we investigated whether fluid flow continues along the western segment of the SWIM1 fault (or Lineament South; Duarte et al., 2011) across the HAP where, to date, no MVs have been discovered and tectonic deformation is accommodated along the SWIM strike-slip faults only. We present new pore-water data from 10 gravity cores (GCs) and heat-flow surveys along the SWIM1 fault trace performed during R/V *Meteor* cruise M86/5 in 2012 (Fig. 1; Sections S1, S2, and S3 in the Supplemental Material[1]). On the quest for potential fluid-escape sites, a number of cores were taken on top of gentle bathymetric features, which rise as high as 100 m above the otherwise flat surrounding seafloor. Seismic records show that these highs correspond to *en echelon* anticlines forming positive flower structures (FSs) within transpressive fault segments of 4 km to 15 km in length (Figs. 1B and 1C; Rosas et al., 2009;

[1]Supplemental Material. Data tables, description of methods, and numerical model. Please visit https://doi.org/10.1130/GEOL.S.16807072 to access the supplemental material, and contact editing@geosociety.org with any questions.

CITATION: Hensen, C., et al., 2021, Oceanic strike-slip faults represent active fluid conduits in the abyssal sub-seafloor: Geology, v. XX, p. , https://doi.org/10.1130/G49344.1

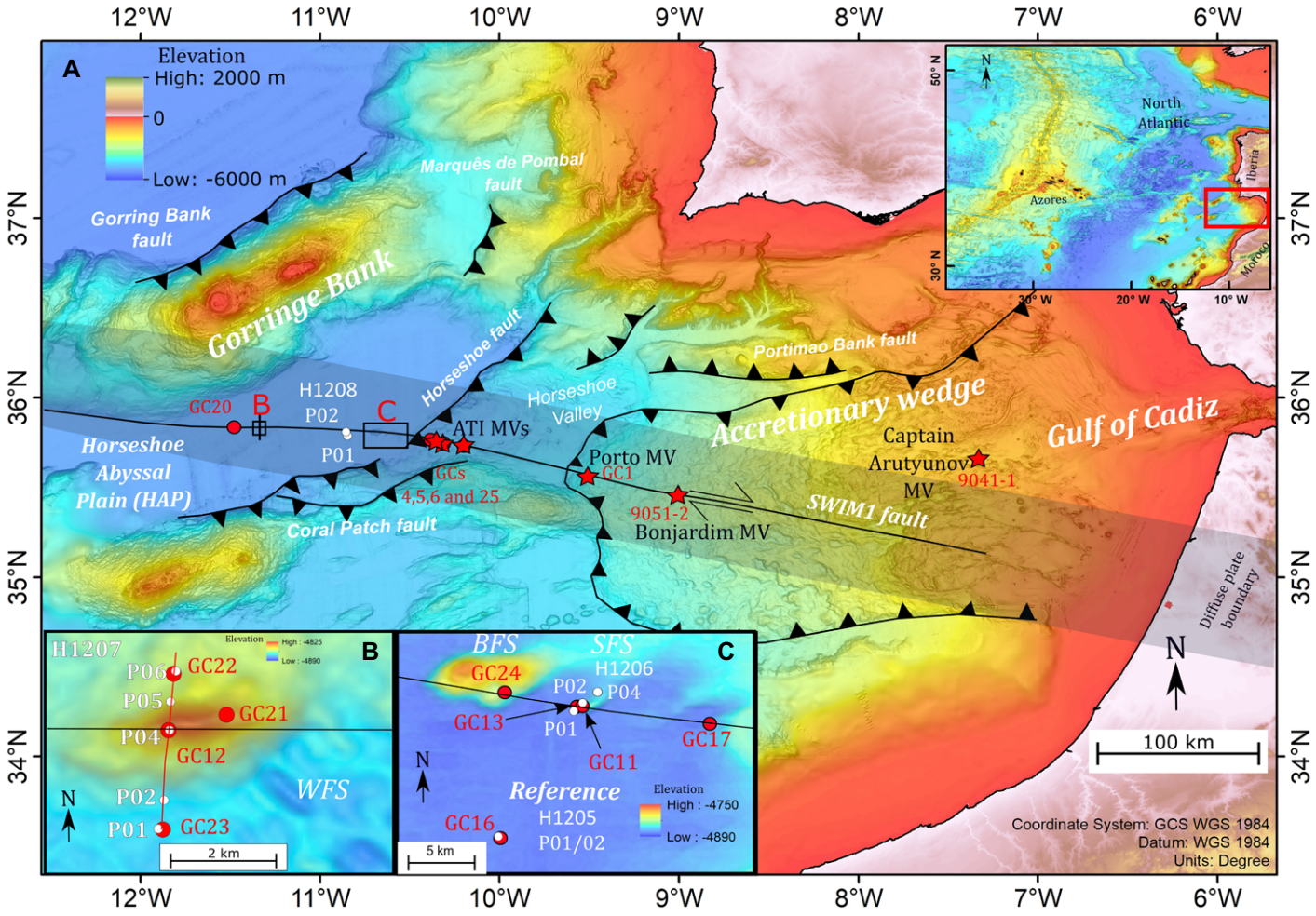

Figure 1. (A) Bathymetric map of the Horseshoe Abyssal Plain and Gulf of Cadiz, northeastern Atlantic Ocean (Zitellini et al., 2009), with sites of gravity cores (GC, red dots) and heat-flow measurements (P0x, white dots). Mud volcanoes (MVs) are shown as red stars. ATI—Abzu–Tiamat–Michael Ivanov; SWIM—southwest Iberian margin; WGS—World Geodetic System. Seafloor hills above flower structures (FSs) are shown in inset maps: western FS (WFS) (B); big and small FSs (BFS and SFS) (C). Red line in B depicts location of transect across the WFS shown in Figure 4.

Martínez-Loriente et al., 2013) associated with upward-diverging deep-seated faults (Harding, 1985; Storti et al., 2003). Our findings provide evidence for active upward fluid flow within these structures and highlight the significance of strike-slip fault zones as fluid pathways.

EVIDENCE FOR FLUID FLOW

Pore water profiles of chloride (Cl), methane (CH_4), sulfate (SO_4), magnesium (Mg), and strontium (Sr) from 10 GCs sampled along the SWIM1 fault in the HAP (Fig. 1; Sections S1 and S2) are shown in Figures 2A and 2B along with concentration profiles from MVs for comparison (Fig. 2C; Sections S4 and S5; Hensen et al., 2015). All sites are located on or close to the SWIM1 fault trace except for the reference core (GC16; Fig. 1), which is located 10 km south of the fault in a place without indications for tectonic activity. Morphologically, the SWIM1 fault trace is essentially inapparent in the bathymetric map of the HAP, but there are bathymetric elevations where FSs have formed in the subsurface (Fig. 1; Martínez-Loriente et al., 2013): the western (WFS), big (BFS), and small flower structure (SFS). Pore-water profiles from cores sampled on top of these FSs (Fig. 2A) reveal significantly steeper concentration gradients of Sr, Mg, and SO_4 as well as higher concentrations of CH_4 compared to profiles from non-FS locations (Fig. 2B). Cores shown in Figure 2B are either from the fault trace without a FS underneath (GC17 and GC20) or taken at some distance from the SWIM1 fault trace (GC22 and GC23, WFS transect; Fig. 1B).

The trends in Figure 2A are, except for chloride, very similar to those observed at MVs (Fig. 2C), suggesting that the same underlying processes are involved (Hensen et al., 2007; Scholz et al., 2009, 2013): (1) SO_4 consumption is predominantly driven by anaerobic oxidation of methane (AOM), while SO_4 reduction in surface sediments is of minor importance; (2) the loss of Mg can be explained by various processes such as co-precipitation during AOM-induced authigenic carbonate formation, dolomite formation, the formation of Mg-rich clay minerals, or a crustal sink; and (3) there are two major sources of Sr to the pore water, the recrystallization of Upper Jurassic carbonates (predominant at distal ATI MVs) and illitization (predominant at nearshore MVs).

The Sr geochemistry has been analyzed by using selected pore-water samples from FSs with a positive Sr excursion (Fig. 2A) along with data from MVs (Hensen et al., 2007, 2015). Although strongly diluted, the FS samples plot on a mixing line between present-day seawater and the average concentration of ATI MVs (Fig. 3A). Sr enrichments at proximal MVs (Bonjardim, Captain Arutyunov) indicate a more radiogenic Sr source related to illitization (Hensen et al., 2015). This result suggests that the excess Sr at the FS sites predominantly stems from recrystallization of carbonates, which have been assigned to Upper Jurassic age for the ATI MV sites (Hensen et al., 2015). The age of the basement in the HAP, which largely consists of exhumed mantle, has been dated from Upper Jurassic (Ramos et al., 2017) to Lower Cretaceous (Martínez-Loriente et al., 2013). This implies a larger range for the

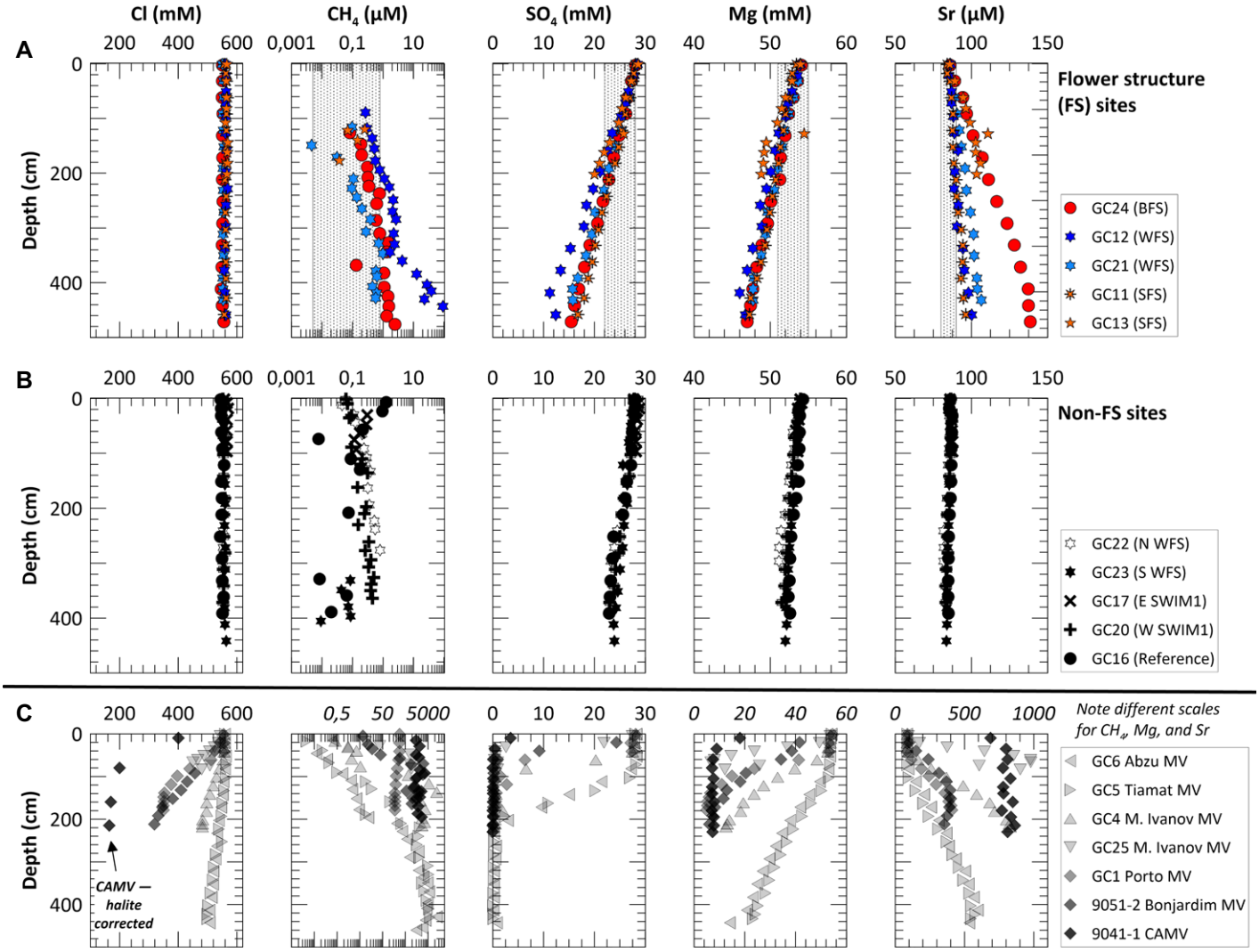

Figure 2. Pore-water profiles from cores sampled on top of flower structures (FSs) along the SWIM1 fault (Horseshoe Abyssal Plainm northeastern Atlantic Ocean) show pronounced concentration gradients versus depth for SO_4, Mg, and Sr (A). Cores from non-FS sites show weaker gradients and lack Sr enrichments (B). Shaded areas in A depict concentration ranges of CH_4, SO_4, Mg, and Sr for stations in B. For comparison, pore-water data from Abzu–Tiamat–Michael (M.) Ivanov, Porto, Bonjardim, and Captain Arutyunov (CAMV) mud volcanoes (MVs) are presented (C). Data for the Bonjardim MV and CAMV are from Hensen et al. (2007).

maximum age and thus the $^{87}Sr/^{86}Sr$ values of the carbonates (Fig. 3A). Regardless of the precise age, the isotopic signature suggests a deep source of the fluids from the base of the sedimentary record, which is located at a maximum depth of 2.5–5 km in the vicinity of the SWIM1 fault (Martínez-Loriente et al., 2013).

Source rocks and source depth of Sr seem to be in line with those of CH_4, which has been shown to be thermogenic at nearly all MV sites. Source-rock temperatures for CH_4 generation in Upper Jurassic to Lower Cretaceous facies were estimated to be in the range of 60–200 °C for the ATI and Porto MVs (Nuzzo et al., 2019). In the HAP, these formations are located within ~2–5 km depth corresponding to a temperature range roughly between 45 and 110 °C (assuming a heat flow of 45 mW m^{-2} and a thermal conductivity of 2 W K^{-1} m^{-1} for the sediment section). The reason for the Mg depletion is less well constrained because there are different possibilities for underlying processes. The advection of crustal-derived fluids or dolomitization of carbonate units would also imply a deep fluid source. However, weak Mg depletion is visible also at non-FS sites (Fig. 2B) where advection is absent, implying that Mg is also depleted at shallower levels (e.g., due to AOM).

It is important to note that the typical freshening signal from illitization (Cl depletion at MV sites) is lacking at the FSs (Figs. 2A and 2C). As mentioned before, illitization decreases from east to west throughout the Gulf of Cadiz as the terrigenous Paleogene units decrease in thickness in the same direction (Scholz et al., 2010). These units cover the uppermost ~3 km below seafloor in the HAP (Martínez-Loriente et al., 2013), which, for a basal heat flow of ~45 mW m^{-2}, results in a maximum temperature of <70 °C. This temperature is insufficient to reach a considerable level of illitization (occurring at 60–150 °C; e.g., Hensen et al., 2015). This fact explains not only the absence of pore-water freshening but also missing enrichments of other fluid-mobile elements such as B and Li. We argue that it is also the reason for the general absence of mud volcanism in the Horseshoe Abyssal Plain.

Steeper SO_4 gradients and higher CH_4 levels at FS sites (Fig. 2A) suggest that there is a significantly higher CH_4 flux at FSs along the fault line compared to non-FS sites (Fig. 2B) (e.g., Borowski et al., 1996). Extrapolation of the SO_4 gradients suggests a minimum depth of SO_4 depletion at 6–10 m below seafloor, which is much deeper than at ATI MVs, implying much lower flow velocities at the FS sites compared to the MVs.

To evaluate if and to what extent the profiles (Fig. 2A) are affected by upward advection, we developed a one-dimensional transport-reaction model considering pore-water transport of dissolved SO_4, CH_4, Sr, and Mg driven by sediment burial, compaction, upward advection, molecular diffusion, as well as the reaction

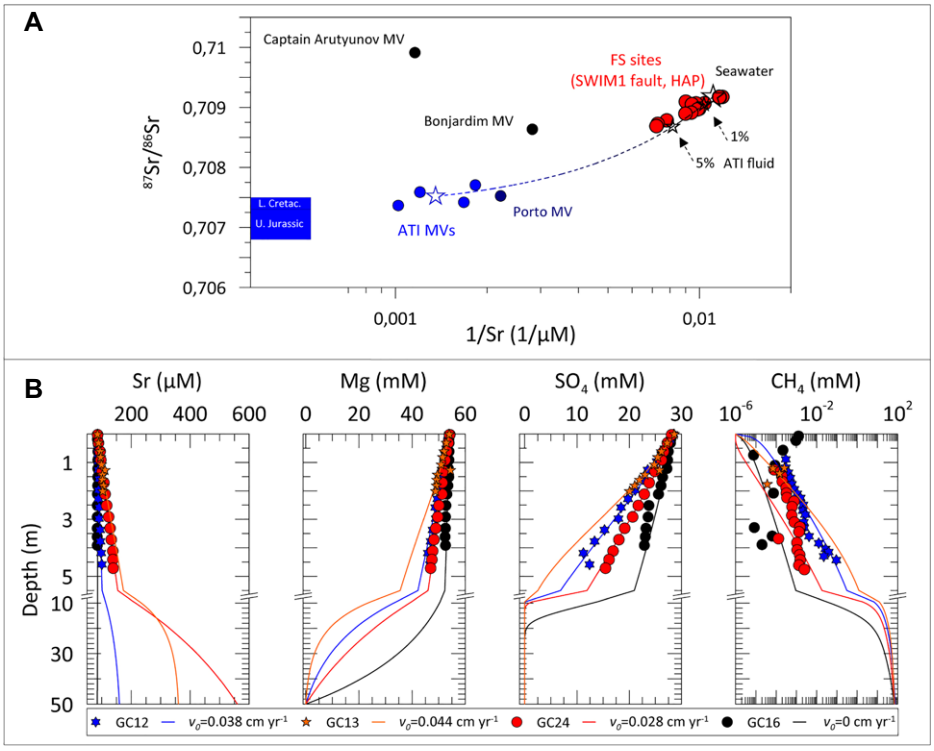

Figure 3. (A) Plot of $^{87}Sr/^{86}Sr$ versus 1/Sr of selected end members from flower structures (FS) and mud volcano (MV) sites (Figs. 2A and 2C). Stippled line indicates two-endmember mixing between present-day seawater (large open black star) and the average composition of pore fluids at Abzu–Tiamat–Michael Ivanov (ATI) MVs (open blue star). Small stars correspond to the 1% and 5% fractions of the ATI fluid. Upper Jurassic to Lower Cretaceous $^{87}Sr/^{86}Sr$ paleo-seawater ratios (Banner, 2004) are indicated by blue box. HAP—Horseshoe Abyssal Plain. (B) Results of reactive-transport model for selected sites at the western, big, and small FSs (WFS, BFS, and SFS, respectively) as well as reference station GC16. Dots are measured pore-water concentrations; solid lines are model results; v_0 is imposed upward fluid-flow velocity at sediment surface.

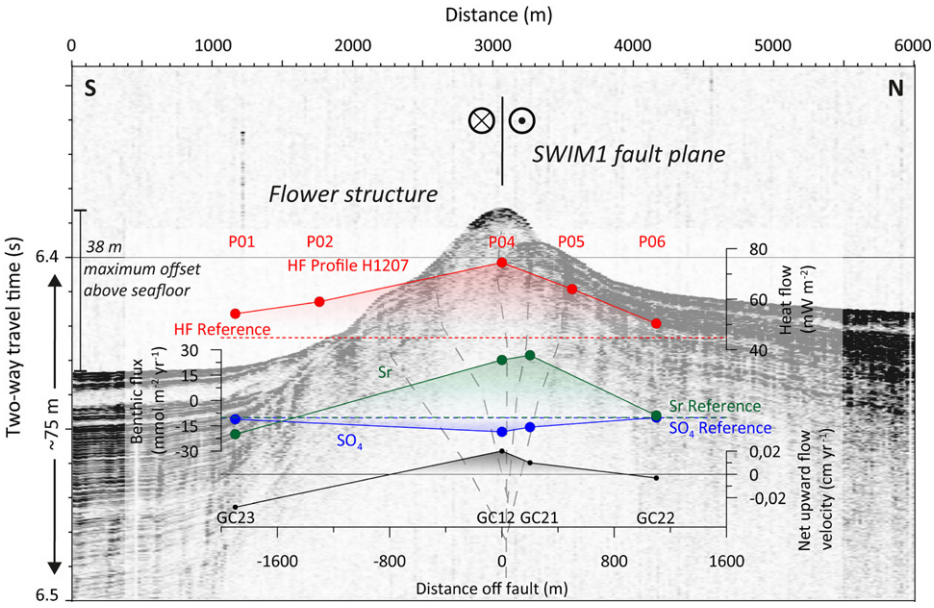

Figure 4. Cross-fault transect of seismic (Parasound sub-bottom profiler) data across the SWIM1 fault at the western flower structure. Gray dashed lines indicate upward diverging faults. Heat flow (HF), model-derived benthic fluxes of SO_4 and Sr, as well as net advective fluxes (= upward fluid flow + compaction – pore water burial) are shown as an overlay (horizontal axis to scale). See Figure 1 for site locations. Negative fluxes are directed into the sediment; positive fluxes are directed out of the sediment. Reference values refer to data at the reference stations (GC16 for SO_4 and Sr; HF1205 P01/02 for heat flow).

of SO_4 and CH_4 by AOM (cf. Section S6 of the Supplemental Material for details). To constrain relevant transport mechanisms, it was crucial to provide a largely realistic model parametrization and boundary conditions for a standard case at the reference site (GC16). A general problem is to define a realistic CH_4 concentration at the lower boundary of the model, given that it intrinsically determines the location of the AOM zone and the steepness of the SO_4 gradients above (Borowski et al., 1996). This value was approximated by calculating the CH_4 solubility with respect to CH_4 hydrate (Tishchenko et al., 2005) considering ambient pressure and temperature conditions. By choosing a column length of 50 m and applying a bulk sedimentation rate based on Gràcia et al. (2010), we were able to fit the model to measured data of site GC16 (Fig. 3B; Section S7). Using the standard parametrization for sedimentation rate and column length and adapting to site-specific differences (e.g., porosity, lower boundary CH_4 concentration, etc.) for the stations along the SWIM1 fault and imposing an upward-directed flow velocity, it was possible to fit the model to the data in all cases. Examples are presented for each of the studied FSs (sites GC12, GC13, GC24; Fig. 3B; Section S7). The imposed velocities (v_0, ranging from 0.028 to 0.044 cm yr^{-1}) result in a concomitant fit of SO_4 and Mg profiles without further adaption of parameters, which makes a strong argument for upward advection of CH_4-rich and Mg-depleted (0 mM) fluids as the predominant process shaping the observed pore-water profiles. Sr concentrations at the lower boundary were chosen to fit the measured profiles in each case (Fig. 3B). Lower values at the WFS indicate a weaker Sr source strength at depth toward the western end of the SWIM1 fault.

The evidence for upward fluid flow at the FSs is further corroborated by increased heat flow at the FSs (Sections S3 and S8), which can be correlated to element fluxes across the seafloor calculated from the numerical model output. The results are presented as cross-sections on top of the seismic record for the WFS (Fig. 4). The central part of the FS is characterized by the highest heat flow and element fluxes as well as average net upward fluid-flow velocities of 0.015 cm yr^{-1} (Fig. 4). On average, for all investigated sites, the fluid flow at FSs (Fig. 2A) imposes an average Sr flux of 37 µmol m^{-2} yr^{-1} and results in an enhanced SO_4 consumption (−16 mmol m^{-2} yr^{-1}). All non-FS sites (Fig. 2B) are sinks for Sr (−10 µmol m^{-2} yr^{-1}) and average SO_4 fluxes (−10 mmol m^{-2} yr^{-1}) are 40% lower than at the FS sites (Fig. 4; Section S9). Due to the upward flow component at the FS sites, the average Mg loss (−1.5 mmol m^{-2} yr^{-1}) is ~5× lower than at non-FS sites (−8.1 mmol m^{-2} yr^{-1}).

IMPLICATIONS

At the SWIM1 fault, fluids sampled at FSs receive their Sr geochemical imprint from the

oldest carbonate units on top of the basement. These units are improbable fluid sources due to the lack of mineral-bound water, which is typically found in terrigenous sedimentary units. For the Porto MV, a deeper source of fluids, the underlying oceanic crust, could be deduced from geochemical data (Hensen et al., 2015). Crustal flow could be triggered by a functional interaction between high relict permeability in old oceanic crust (Johnson, 1980) and development of high-permeability conduits along the deep-cutting fault zone. In any case, if existent in the Horseshoe Abyssal Plain, the geochemical impact of crustal flow must be weak and masked by geochemical processes in sediments above.

Structurally, these FSs are fault-controlled anticline folds, which are associated with strike-slip restraining bends along the SWIM1 fault (Rosas et al., 2009). Positive FSs indicate transpression; i.e., shortening across the main strike-slip fault. The transition from off-FS into the FS shown in the subbottom profile (Fig. 4) illustrates that packages of layers are thinned and faulted. This favors an increase of brittleness, secondary porosity, and permeability within positive FSs and may explain the observed upward fluid flow along the fault plane as observed by geochemical and geophysical methods.

High-resolution bathymetric data (Zitellini et al., 2009) show that the occurrence of FSs in the HAP is not restricted to the SWIM1 fault. Worldwide, complex FSs have been reported from places such as the northern Caribbean plate boundary, which is a >1500-km-long strike-slip fault zone cutting through continental and oceanic lithosphere (Wessels, 2019). FSs are generally abundant in regions of fault bends and stepovers in strike-slip environments (Storti et al., 2003). Our study provides the first complementary data set of geochemical porewater and heat-flow data from FSs related to anticlinal folds, indicating that they represent a hitherto largely unrecognized pathway for solutes to the ocean. More widespread, cross-disciplinary investigations of oceanic strike-slip faults are needed to evaluate the general relevance of our findings with regard to solute and heat exchange between the lithosphere and the deep ocean (Hensen et al., 2019).

ACKNOWLEDGMENTS

Our thanks go to J. Gieskes and five anonymous reviewers, as well as to our colleagues A. Bleyer, B. Domeyer, A. Kolevica, and R. Surberg. Funding of this study was from TransFlux, ICONOX (both German Research Foundation [DFG]); and the ES1301 project (European Cooperation in Science and Technology [COST]).

REFERENCES CITED

Banner, J.L., 2004, Radiogenic isotopes: Systematics and applications to Earth surface processes and chemical stratigraphy: Earth-Science Reviews, v. 65, p. 141–194, https://doi.org/10.1016/S0012-8252(03)00086-2.

Borowski, W.S., Paull, C.K., and Ussler, W., III, 1996, Marine pore-water sulfate profiles indicate in situ methane flux from underlying gas hydrate: Geology, v. 24, p. 655–658, https://doi.org/10.1130/0091-7613(1996)024<0655:MPWSPI>2.3.CO;2.

Duarte, J.C., Rosas, F.M., Terrinha, P., Gutscher, M.-A., Malavieille, J., Silva, S., and Matias, L., 2011, Thrust-wrench interference tectonics in the Gulf of Cadiz (Africa-Iberia plate boundary in the North-East Atlantic): Insights from analog models: Marine Geology, v. 289, p. 135–149, https://doi.org/10.1016/j.margeo.2011.09.014.

Gràcia, E., Vizcaino, A., Escutia, C., Asioli, A., Rodés, Á., Pallàs, R., Garcia-Orellana, J., Lebreiro, S., and Goldfinger, C., 2010, Holocene earthquake record offshore Portugal (SW Iberia): Testing turbidite paleoseismology in a slow-convergence margin: Quaternary Science Reviews, v. 29, p. 1156–1172, https://doi.org/10.1016/j.quascirev.2010.01.010.

Haffert, L., et al., 2013, Fluid evolution and authigenic mineral paragenesis related to salt diapirism—The Mercator mud volcano in the Gulf of Cadiz: Geochimica et Cosmochimica Acta, v. 106, p. 261–286, https://doi.org/10.1016/j.gca.2012.12.016.

Harding, T.P., 1985, Seismic characteristics and identification of negative flower structures, positive flower structures and positive structural inversion: American Association of Petroleum Geologists Bulletin, v. 69, p. 582–600, https://doi.org/10.1306/AD462538-16F7-11D7-8645000102C1865D.

Hensen, C., Nuzzo, M., Hornibrook, E., Pinheiro, L.M., Bock, B., Magalhães, V.H., and Brückmann, W., 2007, Sources of mud volcano fluids in the Gulf of Cadiz—Indications for hydrothermal imprint: Geochimica et Cosmochimica Acta, v. 71, p. 1232–1248, https://doi.org/10.1016/j.gca.2006.11.022.

Hensen, C., et al., 2015, Strike-slip faults mediate the rise of crustal-derived fluids and mud volcanism in the deep sea: Geology, v. 43, p. 339–342, https://doi.org/10.1130/G36359.1.

Hensen, C., et al., 2019, Marine transform faults and fracture zones: A joint perspective integrating seismicity, fluid flow and life: Frontiers of Earth Science, v. 7, 39, https://doi.org/10.3389/feart.2019.00039.

Johnson, D.M., 1980, Crack distribution in the upper oceanic crust and its effects upon seismic velocity, seismic structure, formation permeability, and fluid circulation, *in* Donnelly, T.W., and Francheteau, J., eds., Initial Reports of the Deep Sea Drilling Project, Volume 51/52/53: Washington, D.C., U.S. Government Printing Office, p. 1479–1490.

Magalhães, V.H., et al., 2012, Formation processes of methane-derived authigenic carbonates from the Gulf of Cadiz: Sedimentary Geology, v. 243–244, p. 155–168, https://doi.org/10.1016/j.sedgeo.2011.10.013.

Martínez-Loriente, S., et al., 2013, Active deformation in old oceanic lithosphere and significance for earthquake hazard: Seismic imaging of the Coral Patch Ridge area and neighboring abyssal plains (SW Iberian Margin): Geochemistry Geophysics Geosystems, v. 14, p. 2206–2231, https://doi.org/10.1002/ggge.20173.

Nuzzo, M., et al., 2019, Formation and migration of hydrocarbons in deeply buried sediments of the Gulf of Cadiz convergent plate boundary—Insights from the hydrocarbon and helium isotope geochemistry of mud volcano fluids: Marine Geology, v. 410, p. 56–69, https://doi.org/10.1016/j.margeo.2019.01.005.

Ramos, A., Fernández, O., Torne, M., Sánchez de la Muela, A., Muñoz, J.A., Terrinha, P., Manatschal, G., and Salas, M.C., 2017, Crustal structure of the SW Iberian passive margin: The westernmost remnant of the Ligurian Tethys?: Tectonophysics, v. 705, p. 42–62, https://doi.org/10.1016/j.tecto.2017.03.012.

Rosas, F.M., Duarte, J.C., Terrinha, P., Valadares, V., and Matias, L., 2009, Morphotectonic characterization of major bathymetric lineaments in Gulf of Cadiz (Africa-Iberia plate boundary): Insights from analogue modelling experiments: Marine Geology, v. 261, p. 33–47, https://doi.org/10.1016/j.margeo.2008.08.002.

Schmidt, C., Burwicz, E., Hensen, C., Wallmann, K., Martínez-Loriente, S., and Gràcia, E., 2018, Genesis of mud volcano fluids in the Gulf of Cadiz using a novel basin-scale model approach: Geochimica et Cosmochimica Acta, v. 243, p. 186–204, https://doi.org/10.1016/j.gca.2018.09.011.

Scholz, F., Hensen, C., Reitz, A., Romer, R.L., Liebetrau, V., Meixner, A., Weise, S.M., and Haeckel, M., 2009, Isotopic evidence ($^{87}Sr/^{86}Sr$, $\delta^{7}Li$) for alteration of the oceanic crust at deep-rooted mud volcanoes in the Gulf of Cadiz, NE Atlantic Ocean: Geochimica et Cosmochimica Acta, v. 73, p. 5444–5459, https://doi.org/10.1016/j.gca.2009.06.004.

Scholz, F., Hensen, C., Lu, Z., and Fehn, U., 2010, Controls on the $^{129}I/I$ ratio of deep-seated marine interstitial fluids: 'Old' organic versus fissiogenic ^{129}I: Earth and Planetary Science Letters, v. 294, p. 27–36, https://doi.org/10.1016/j.epsl.2010.02.034.

Scholz, F., Hensen, C., Schmidt, M., and Geersen, J., 2013, Submarine weathering of silicate minerals and the extent of pore water freshening at active continental margins: Geochimica et Cosmochimica Acta, v. 100, p. 200–216, https://doi.org/10.1016/j.gca.2012.09.043.

Storti, F., Holdsdworth, R.E., and Salvini, F., 2003, Intraplate strike-slip deformation belts, *in* Storti, F., et al., eds., Intraplate Strike-Slip Deformation Belts: Geological Society [London] Special Publication 210, p. 1–14, https://doi.org/10.1144/GSL.SP.2003.210.01.01.

Terrinha, P., et al., 2009, Morphotectonics and strain partitioning at the Iberian-Africa plate boundary from multibeam and seismic reflection data: Marine Geology, v. 267, p. 156–174, https://doi.org/10.1016/j.margeo.2009.09.012.

Tishchenko, P., Hensen, C., Wallmann, K., and Wong, C.S., 2005, Calculation of the stability and solubility of methane hydrate in seawater: Chemical Geology, v. 219, p. 37–52, https://doi.org/10.1016/j.chemgeo.2005.02.008.

Vanneste, H., Kelly-Gerreyn, B.A., Connelly, D.P., James, R.H., Haeckel, M., Fisher, R.E., Heeschen, K.U., and Mills, R.A., 2011, Spatial variation in fluid flow and geochemical fluxes across the sediment-seawater interface at the Carlos Ribeiro mud volcano (Gulf of Cadiz): Geochimica et Cosmochimica Acta, v. 75, p. 1124–1144, https://doi.org/10.1016/j.gca.2010.11.017.

Wessels, R.J.F., 2019, Strike-slip fault systems along the northern Caribbean plate boundary, *in* Duarte, J. C., ed., Transform Plate Boundaries and Fracture Zones: Amsterdam, Elsevier, p. 375–395, https://doi.org/10.1016/B978-0-12-812064-4.00015-3.

Zitellini, N., et al., 2009, The quest for the Africa-Eurasia plate boundary west of the Strait of Gibraltar: Earth and Planetary Science Letters, v. 280, p. 13–50, https://doi.org/10.1016/j.epsl.2008.12.005.

Printed in USA